Case Studies in Nondestructive Testing and Evaluation 3 (2015) 1–8

Contents lists available at ScienceDirect

Case Studies in Nondestructive Testing and Evaluation

www.elsevier.com/locate/csndt

Case study of guided wave propagation in a one-side water-immersed steel plate

Lingyu Yu, Zhenhua Tian *

Department of Mechanical Engineering, University of South Carolina, 300 Main St., Columbia, SC 29208, USA

ARTICLE INFO

Article history:
Available online 16 December 2014

ABSTRACT

This paper presents a case study of guided waves in a steel plate with one side immersed in water. A hybrid sensing system that uses PZT as the guided wave actuator and a scanning laser vibrometer as the guided wave receiver is employed to acquire the time–space wavefield data. By using the two dimensional Fourier transform, the time–space wavefield is transformed into the frequency–wavenumber domain where the wave modes and the guided wave dispersion can be determined. The study confirms the existence of quasi-Scholte wave in the one-sidedly water-immersed plate in addition to fundamental guided waves. The results also show the quasi-Scholte wave can be directly generated and measured in the immersed plate at low frequencies using the present sensing system. Through pitch–catch sensing tests, the influence of water on guided wave propagation in the one-side water-immersed plate is investigated. It is seen that the water level affects the wave propagation time linearly and can be potentially used for estimation of water level in a container.

1. Introduction

Nondestructive evaluation (NDE) and structural health monitoring (SHM) of thin-wall structures using guided waves are based on the understanding of wave propagation and interactions within the structural waveguide [1–10]. Guided waves have been used for inspection in immersed structures, such as ship hulls, submarines and underwater pipes [11–16] with focuses on detecting structural discontinuities in such immersed structures. Nonetheless, using guided waves for evaluating plate surface condition change due to the presence of water is much less discussed. When a free plate is immersed in water, the guided wave propagation in the plate will be affected. The out-of-plane motion in the plate will transmit into the water through the plate–water interface [2]. The surrounding water provides a way for the guided wave energy to leak outwards from the plate known as leaky guided waves [2]. Compared to the guided waves in the free plate, the leaky guided waves in the immersed plate have different behaviors, such as mode shapes, wave speeds and attenuations [17–23].

Besides the leaky guided waves, there is another wave mode reported by Cegla et al. known as quasi-Scholte mode present in the immersed plate [21,22]. The authors studied the quasi-Scholte wave in a plate with both sides immersed in infinite fluid, where the plate is considered as a symmetrically loaded waveguide [21]. It is found the quasi-Scholte wave is dispersive at low frequencies and asymptotes to the nondispersive Scholte wave behavior at high frequencies [21]. Also

* Corresponding author. Tel.: +1 8037776660.
E-mail address: tian@email.sc.edu (Z. Tian).

http://dx.doi.org/10.1016/j.csndt.2014.11.001

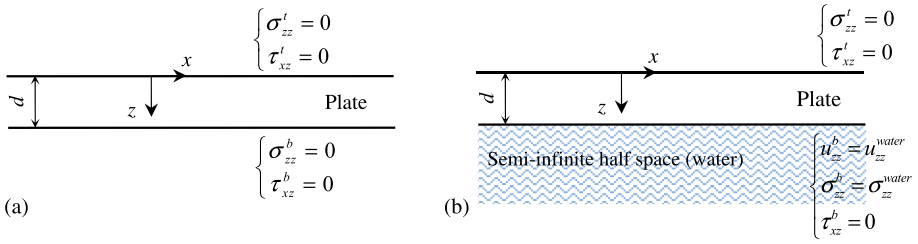

Fig. 1. Sketches for: (a) free plate, and (b) plate with one side in water.

at low frequencies the quasi-Scholte wave energy predominantly flows in the plate, while at high frequencies most of the energy is in the fluid [21].

This paper presents an experimental investigation of the case of guided waves including the quasi-Scholte wave in a plate with only one side immersed in water. The study is enabled by the time–space wavefield acquired by a scanning laser vibrometer and the use of 2D Fourier transform (FT) to convert the wavefield to the frequency–wavenumber representation, by which the characteristics of the guided wave modes as well as the quasi-Scholte mode can be easily identified and analyzed. The effects of water level on wave propagation are also investigated. The paper is organized as follows. Section 2 presents the theoretical prediction of guided wave propagation in the one-side water-immersed plate. Section 3 gives the experimental setup and the wave propagation characterization by the use of the 2D FT. The water level influence on wave propagation is also investigated by analyzing the traveling time of the wave signals. The paper is finally concluded with discussions in Section 4.

2. Guided waves in a one-side water-immersed plate

The classical problem of guided wave propagation in a traction-free isotropic plate has been thoroughly studied and can be found in many references such as [2,3,24,25]. For the completeness of knowledge we provide a brief derivation of dispersion curves of guided waves in a plate with one side in water. The dispersion curves will also be used for the case study in Section 3.

In a free plate (Fig. 1(a)), with traction-free boundary conditions, its characteristic equation can be derived and expressed as [2,3,25]:

$$\begin{vmatrix} k_S^2-\xi^2 & k_S^2-\xi^2 & -2k_S\xi & 2k_S\xi \\ 2k_L\xi & -2k_L\xi & k_S^2-\xi^2 & k_S^2-\xi^2 \\ (k_S^2-\xi^2)g_L & \frac{k_S^2-\xi^2}{g_L} & -2k_S\xi g_S & \frac{2k_S\xi}{g_S} \\ 2k_L\xi g_L & \frac{-2k_L\xi}{g_L} & (k_S^2-\xi^2)g_S & \frac{k_S^2-\xi^2}{g_S} \end{vmatrix} = 0 \tag{1}$$

where, $k_L^2 = \frac{\omega^2}{c_L^2} - \xi^2$, $k_S^2 = \frac{\omega^2}{c_S^2} - \xi^2$, $\xi = \frac{2\pi}{\lambda}$,

$$c_L = \sqrt{\frac{2\mu(1-\nu)}{\rho(1-2\nu)}}, \qquad c_S = \sqrt{\frac{\mu}{\rho}}, \qquad g_L = e^{ik_L d}, \qquad g_S = e^{ik_S d}, \qquad d = 2h$$

h, ω, ξ and λ are half plate thickness, circular frequency, wavenumber and wavelength, respectively. c_L and c_S are longitudinal and transverse bulk wave velocities, respectively. ρ, μ and ν are density, shear modulus and Poisson's ratio of the plate, respectively. Solutions to Eq. (1) can be found in many classic references such as [2,3,24,25]. Fig. 2 gives the frequency–wavenumber dispersion curves for a 1.2 mm thickness steel plate (material properties are listed in Table 1), indicating the presence of the fundamental antisymmetric A_0 and symmetric S_0 modes at frequencies lower than 1000 kHz.

When one side of the plate is immersed in water (*plate-half space water* waveguide, as shown in Fig. 1(b)), the top surface of the plate maintains traction-free boundary conditions. On the bottom surface of the plate, wave motions can transmit into the water since the normal displacement u_{zz} and stress σ_{zz} are continuous at the plate–water interface while the shear stress τ_{xz} remains zero at the interface in that water does not support the shear stress. The characteristic equation for the immersed plate can be assembled and expressed as,

$$\begin{vmatrix} k_S^2-\xi^2 & k_S^2-\xi^2 & -2k_S\xi & 2k_S\xi & 0 \\ 2k_L\xi & -2k_L\xi & k_S^2-\xi^2 & k_S^2-\xi^2 & 0 \\ (k_S^2-\xi^2)g_L & \frac{k_S^2-\xi^2}{g_L} & -2k_S\xi g_S & \frac{2k_S\xi}{g_S} & \frac{\omega^2\rho_w}{\mu} \\ 2k_L\xi g_L & \frac{-2k_L\xi}{g_L} & (k_S^2-\xi^2)g_S & \frac{k_S^2-\xi^2}{g_S} & 0 \\ k_L g_L & \frac{-k_L}{g_L} & -\xi g_S & \frac{-\xi}{g_S} & \gamma \end{vmatrix} = 0 \tag{2}$$

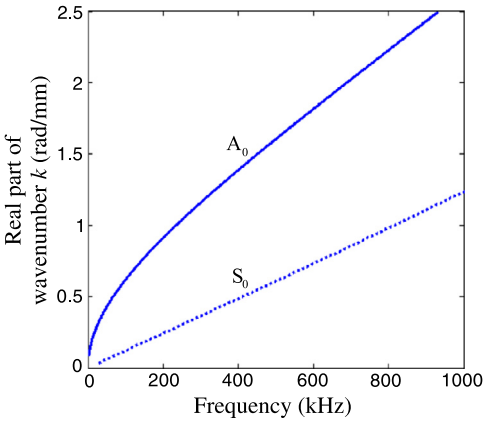

Fig. 2. Wavenumber dispersion curves of a 1.2 mm thickness free steel plate. (Note the imaginary wavenumber of a free plate is zero. Only real part is given.)

Table 1
Material properties.

Steel density (kg/m^3)	8000
Steel Young's modulus (GPa)	196.5
Steel Poisson's ratio	0.29
Steel plate thickness (mm)	1.2
Water density (kg/m^3)	1000
Water bulk wave velocity (m/s)	1500

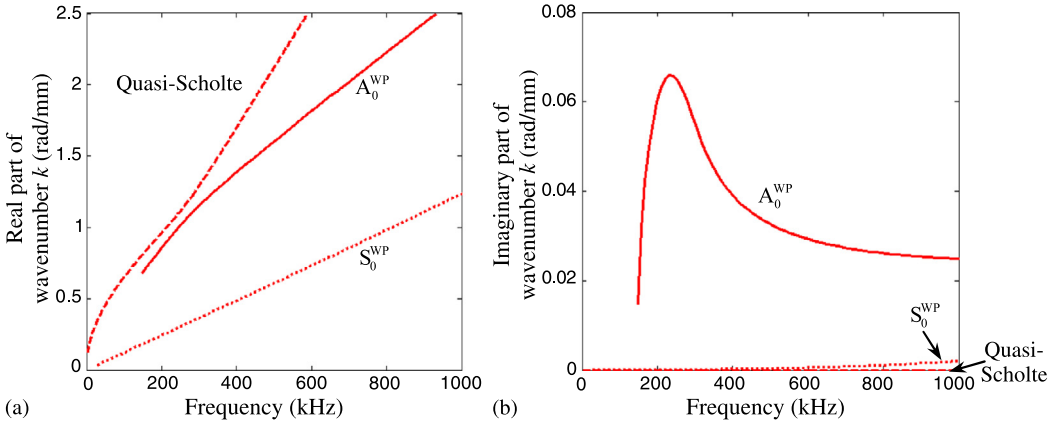

Fig. 3. Wavenumber dispersion curves of a 1.2 mm thickness steel plate with one side in contact with water: (a) real part wavenumber curves, (b) imaginary part wavenumber curves.

where,

$$\gamma^2 = \frac{\omega^2}{c_{Lw}^2} - \xi^2, \quad c_{Lw} = \sqrt{\frac{\lambda_w}{\rho_w}}$$

c_{Lw} is the bulk wave velocity in the surrounding water (ρ_w and λ_w are density and bulk stiffness of water). By solving Eq. (2) numerically, the dispersion curves for a 1.2 mm thickness steel plate with one side in water can be obtained (material properties are listed in Table 1). Due to the energy leakage, the wavenumber roots of Eq. (2) have complex values with the real part indicating the wave components and the imaginary part giving the extent of energy attenuation.

Fig. 3(a) plots the real parts of the wavenumber roots for the immersed plate. The fundamental symmetric and anti-symmetric guided wave modes are present, notated as A_0^{WP} and S_0^{WP} to distinguish from these wave modes in the free plate. Furthermore, an additional mode that exhibits the same dispersive behavior as the quasi-Scholte mode discovered in a two-side immersed plate in [21] is observed. The one-side immersed steel plate in this study shows its capability to support the quasi-Scholte mode as well.

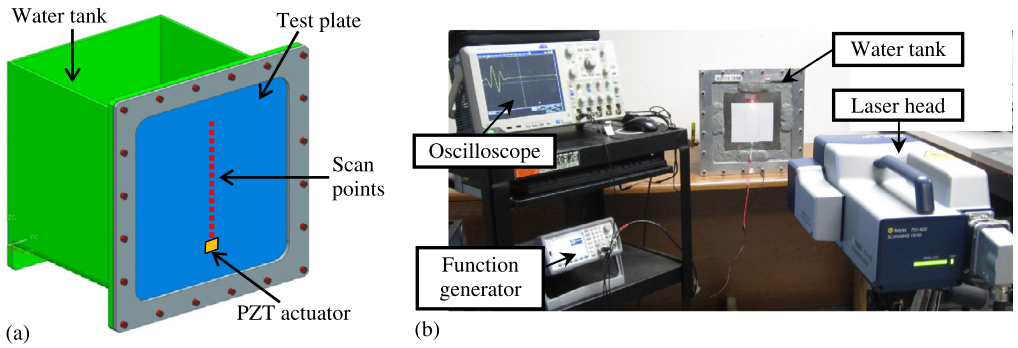

Fig. 4. The hybrid PZT-laser vibrometer sensing experiment: (a) an illustration of the water tank, and (b) the overall test setup.

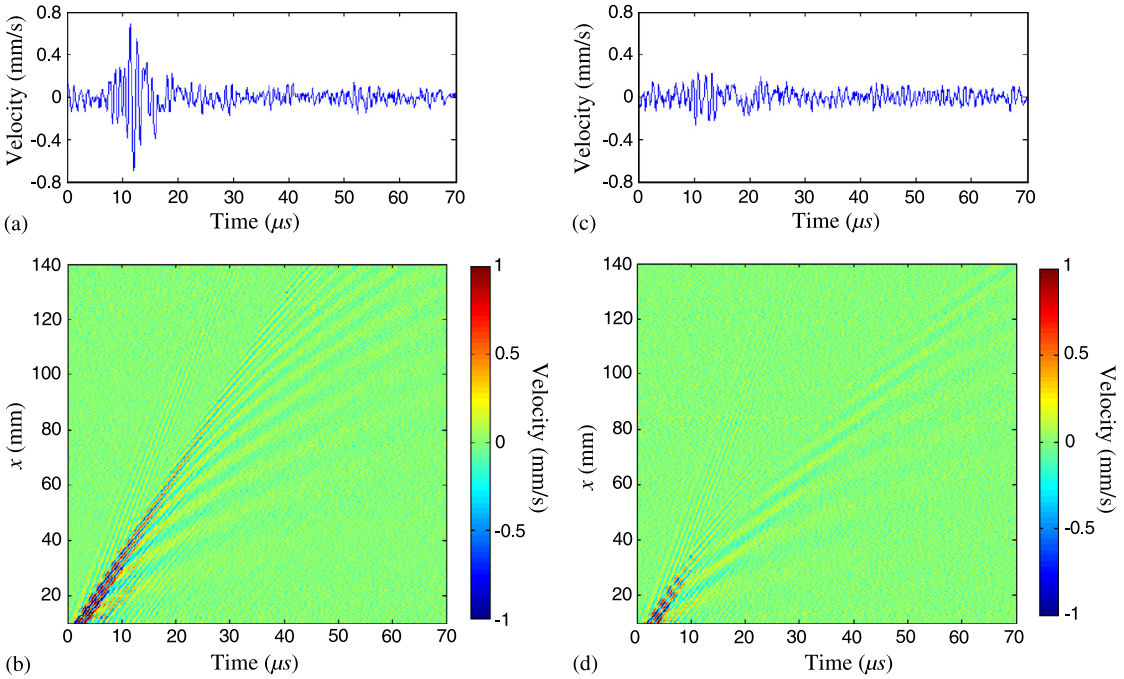

Fig. 5. Laser vibrometry measurements: (a) and (c) are received waveforms at 40 mm away from the source for the free and immersed plates; (b) and (d) are time–space wavefields measured from the free and immersed plates.

3. Wave characterization case study

3.1. Experimental setup

To study the waves in the one-sidedly immersed plate, a test tank (Fig. 4(a)) has been designed with the front wall being removable and replaceable, used as the test plate (a 1.2 mm thickness steel plate with the material properties given in Table 1 in this case). When the tank is empty, the test plate is treated as a free plate; with water in, it is then treated as the immersed plate. A PZT wafer (7 mm × 7 mm square, 0.2 mm thickness, APC850 type) is bonded close to the bottom of the plate as the wave actuator. A coordinate x is defined with the origin O being set at the center of the PZT and vertically upward. Fig. 4(b) shows the overall experimental setup. Time–space wavefields are measured by a scanning laser Doppler vibrometer (SLDV) (model: Polytec PSV-400). The SLDV can measure the particle velocity along the laser beam in a vibrating object surface [26]. In the test, the laser beam is normal to the plate such that the out-of-plane wave motion is measured.

A pulse signal with 0.5 μs duration and 10 V amplitude was sent to the PZT from an arbitrary function generator (model: Agilent 33500B) to excite guided waves. Waves at multiple scan points along the vertical line from the PZT actuator, as indicated in Fig. 4(a), were measured by the SLDV. The spatial resolution of the scan points was 0.3 mm. Two situations, the free plate and a fully immersed plate (using a full water tank), were tested. Fig. 5(a) and Fig. 5(c) plot the waveforms measured at 40 mm for both cases; and Fig. 5(b) and Fig. 5(d) present the time–space wavefields. It is seen the wave

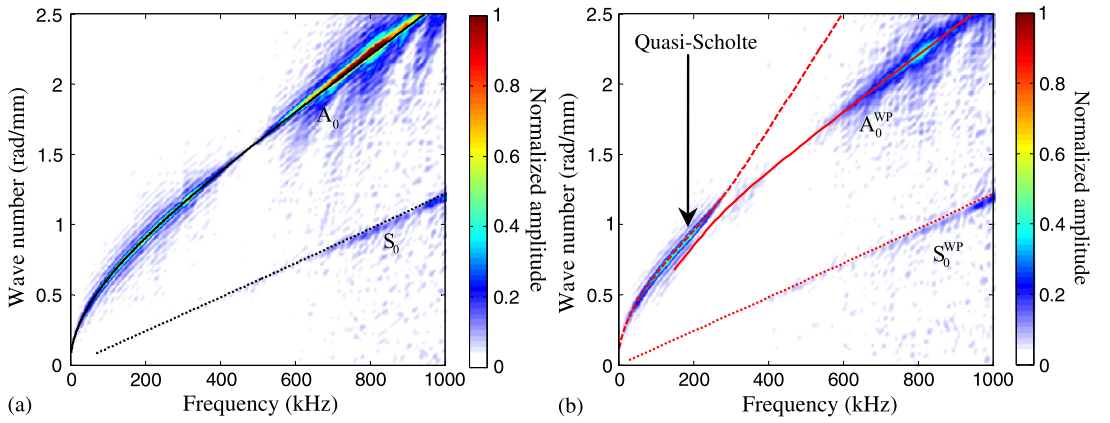

Fig. 6. Frequency–wavenumber analysis results: (a) for the free plate, and (b) for the immersed plate.

propagation in the immersed plate is significantly attenuated. However, it is difficult to determine the wave modes present in each and also difficult to qualitatively and quantitatively tell the differences in the two plates.

3.2. Frequency–wavenumber analysis

The frequency–wavenumber analysis has been reported as an effective means for wave mode identification and wave propagation analysis [26–30]. The frequency–wavenumber representation $U(f,\xi)$ of time–space wavefield data $u(t,x)$ can be obtained by performing the 2D FT, which is defined as [31]:

$$U(f,\xi) = \int_{-\infty}^{\infty}\int_{-\infty}^{\infty} u(t,x)e^{-i(2\pi ft-\xi x)}dtdx \tag{3}$$

where x, ξ, t and f are space, wavenumber, time and frequency variables, respectively.

By using 2D FT, the time–space wavefields for the free and immersed plates are transferred to the frequency–wavenumber domain, as presented in Fig. 6(a) and Fig. 6(b). The theoretical wavenumber dispersion curves are added to the spectra for the purpose of mode identification. In the free plate spectrum, Fig. 6(a), A_0 and S_0 modes are identified. Note that since the out-of-plane motion of A_0 mode is much stronger than that of S_0 mode, the amplitude of A_0 mode in the spectrum is much intensified than that of S_0 mode [26]. Particularly, at frequencies below 500 kHz, the S_0 mode is barely seen due to the very small out-of-plane motion of S_0 mode in this frequency range.

In the immersed plate spectrum, Fig. 6(b), three wave modes including A_0^{WP}, S_0^{WP} and quasi-Scholte modes are discernibly identified. Compared to the free plate case, the spectrum of immersed plate shows that the amplitude of S_0^{WP} mode remains nearly the same as S_0 mode, while the amplitude of A_0^{WP} mode significantly decreases due to the energy leakage. Particularly, at frequencies below 500 kHz, the A_0^{WP} mode nearly disappears. This observation is consistent with the attenuation predicted by the imaginary wavenumber given in Fig. 3(b). Meanwhile, a new wave mode, the quasi-Scholte mode, shows up within the frequency range up to 300 kHz, as reported in [21]. Moreover, the quasi-Scholte mode has slightly different wavenumbers compared to those of the A_0 mode. To clearly show the difference, the free plate spectrum (Fig. 6(a)) was subtracted from the immersed plate spectrum (Fig. 6(b)). The subtraction result and a zoom-in plot are given in Fig. 7. It is noticed in Fig. 7(a) that S_0 mode has been canceled out after the subtraction since S_0 modes are the same at both the immersed and free plates. At lower frequency end, both quasi-Scholte and A_0 mode are remained. The difference plots further confirm that the quasi-Scholte mode in the immersed plate has different wavenumbers compared to those of the A_0 mode in the free plate.

3.3. Water influence on wave propagation

To understand the water influence on the wave propagation, we studied the wave signals acquired at different water levels (d_W) in the tank, from $d_W = 5$ to 135 mm at 10 mm step size. In the test, waves are excited at 100 kHz using a narrowband toneburst and measured at 140 mm away from the actuator at each water level, as illustrated in Fig. 8. As shown in the setup, the wave propagation path (d_{T-R}) consists of the water path d_W, as the immersed plate portion, and the dry path $d_{T-R} - d_W$, as the free plate portion. That's to say, the wave leaves the actuator as the quasi-Scholte mode in the immersed portion d_W, then converts to the A_0 mode in the free portion $d_{T-R} - d_W$. Therefore, the total wave traveling time t_{T-R} can be expressed as

$$t_{T-R} = \frac{d_W}{c_{QS}} + \frac{d_{T-R} - d_W}{c_{A_0}} \tag{4}$$

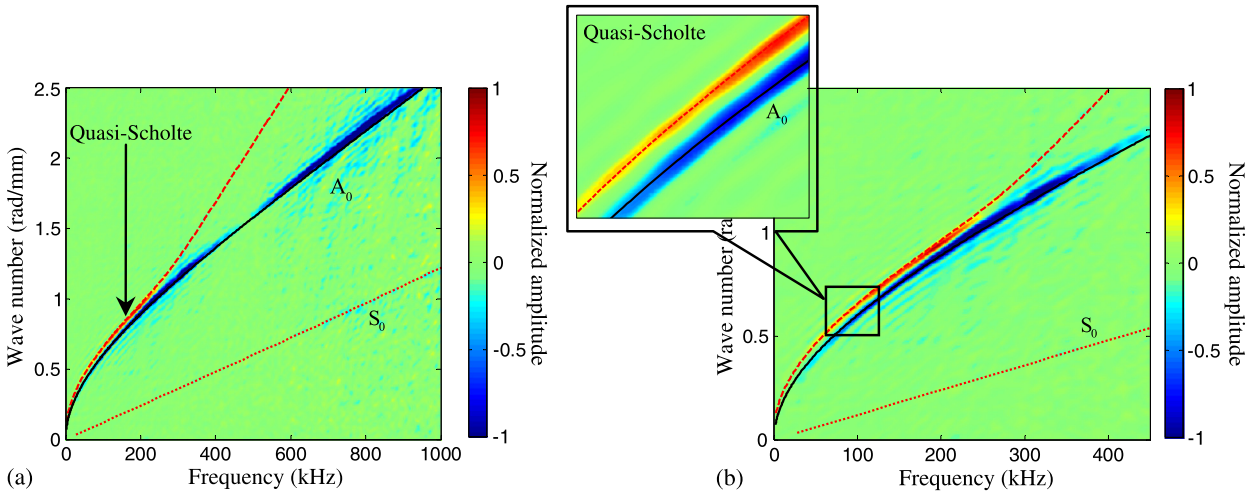

Fig. 7. The spectrum difference obtained by subtracting the free plate spectrum from the immersed plate spectrum: (a) subtraction result, and (b) zoom-in plot of the result.

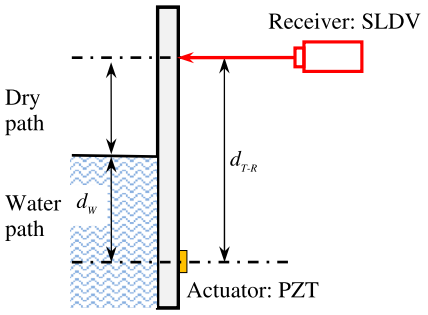

Fig. 8. An illustration of the pitch–catch configuration with the PZT actuator and the SLDV receiver.

where c_{QS} and c_{A_0} are group velocities of the quasi-Scholte mode and the A_0 mode (at 100 kHz, $c_{QS} = 1811$ m/s and $c_{A_0} = 1895$ m/s). Using the free plate when $d_W = 0$ as the baseline, the changes of traveling time at a water level of d_W *w.r.t.* the baseline condition can be derived as

$$\Delta t_{T-R} = d_W \left(\frac{1}{c_{QS}} - \frac{1}{c_{A_0}} \right) \tag{5}$$

Eq. (5) demonstrates a linear relation between the change in traveling time Δt_{T-R} and the water level d_W. The linear relation derived by Eq. (5) is plotted in Fig. 9(a) (solid line).

Experimentally Δt_{T-R} can be acquired from the SLDV measurements. Fig. 9(b) presents the baseline signal (solid line) and the signal at $d_W = 95$ mm (broken line). Please note S_0 mode is not presented in the SLDV measurements. In the baseline signal, the wave packet corresponds to the A_0 mode; while for the $d_W = 95$ mm signal, the wave packet contains both the quasi-Scholte mode from the water path and the A_0 mode from the dry path. The change in traveling time Δt_{T-R} can be readily estimated by calculating the maximum values in the wave packets. For wave signals measured at each water level, the estimated Δt_{T-R} are plotted in Fig. 9 (triangle marker), in comparison to the theoretical prediction (solid line). It is seen the experimental estimation agrees well with the theoretical prediction, validating the linear relationship between the change of traveling time in the wave signals and the water level.

4. Conclusions

In this paper, we presented a case study of guided wave propagation in a plate with one side immersed in water. With the acquisition of time–space wavefield and application of 2D FT, the frequency–wavenumber spectrum is obtained in which the wave modes and the dispersion relation can be discernibly viewed. The analysis also manifests the presence of guided wave modes as well as the quasi-Scholte wave mode in the one-sidedly immersed plate. Below 300 kHz, the quasi-Scholte mode dominates. The investigation of water influence on the wave propagation shows the wave traveling time in a partially immersed plate is determined by the length of the water path and the dry path. A linear relationship between the change of traveling time of the waves and the water level is experimentally confirmed.

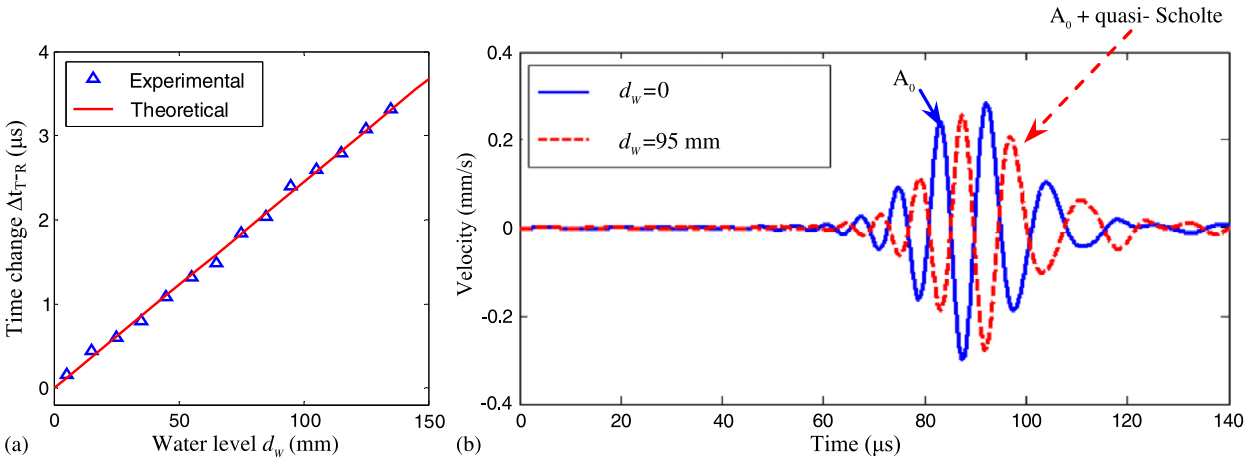

Fig. 9. Water influence on wave propagation at 100 kHz: (a) the relation between the water level and change of traveling time Δt_{T-R}, and (b) received waveforms when water level $d_W = 0$ (solid line) and $d_W = 95$ mm (broken line).

The study also shows that the presented PZT-SLDV system is able to measure the quasi-Scholte wave in the one-sidedly immersed plate. With the measurements the change of traveling time in a plate with certain water level *w.r.t.* the baseline condition can be estimated, and using the linear relationship discovered in this case study, the water level can be derived. This sensing system and methodology can be potentially applied for water level detection in a steel container as reported in [32,33].

Acknowledgement

This work was performed under the support of the US Nuclear Regulatory Commission under the Grant # NRC-04-10-155 “Ultrasonic Guided Wave Sensor for Gas Accumulation Detection in Nuclear Emergency Core Cooling Systems”.

References

[1] Worlton DC. Ultrasonic testing with lamb waves. Nondestruct Test 1957;15:218–22.
[2] Rose JL. Ultrasonic waves in solid media. Cambridge: Cambridge University Press; 1999.
[3] Giurgiutiu V. Structural health monitoring with piezoelectric wafer active sensors. Boston, MA, USA: Academic Press; 2008.
[4] Sohn H, Kim SB. Development of dual PZT transducers for reference-free crack detection in thin plate structures. IEEE Trans Ultrason Ferroelectr Freq Control Jan. 2010;57:229–40.
[5] Di Scalea FL, Salamone S. Temperature effects in ultrasonic lamb wave structural health monitoring systems. J Acoust Soc Am Jul. 2008;124:161–74.
[6] Michaels JE. Detection, localization and characterization of damage in plates with an in situ array of spatially distributed ultrasonic sensors. Smart Mater Struct Jun. 2008;17:035035.
[7] Ihn JB, Chang FK. Pitch–catch active sensing methods in structural health monitoring for aircraft structures. Struct Health Monit Mar. 2008;7:5–19.
[8] Park HW, Sohn H, Law KH, Farrar CR. Time reversal active sensing for health monitoring of a composite plate. J Sound Vib Apr. 2007;302:50–66.
[9] Kundu T. Acoustic source localization. Ultrasonics 2014;54:24–38.
[10] Wilcox PD. Omni-directional guided wave transducer arrays for the rapid inspection of large areas of plate structures. IEEE Trans Ultrason Ferroelectr Freq Control Jun. 2003;50:699–709.
[11] Na WB, Kundu T. Underwater pipeline inspection using guided waves. J Press Vessel Technol 2002;124:196–200.
[12] Bingham J, Hinders M, Friedman A. Lamb wave detection of limpet mines on ship hulls. Ultrasonics Dec. 2009;49:706–22.
[13] Chen JG, Su ZQ, Cheng L. Identification of corrosion damage in submerged structures using fundamental anti-symmetric lamb waves. Smart Mater Struct Jan. 2010;19:015004.
[14] Rizzo P, Han JG, Ni XL. Structural health monitoring of immersed structures by means of guided ultrasonic waves. J Intell Mater Syst Struct Sep. 2010;21:1397–407.
[15] Pistone E, Li KY, Rizzo P. Noncontact monitoring of immersed plates by means of laser-induced ultrasounds. Struct Health Monit Sep. 2013;12:549–65.
[16] Koduru JP, Rose JL. Mode controlled guided wave tomography using annular array transducers for SHM of water loaded plate like structures. Smart Mater Struct Dec. 2013;22:10.
[17] Chimenti DE, Nayfeh AH. Leaky lamb waves in fibrous composite laminates. J Appl Phys 1985;58:4531–8.
[18] Wu J, Zhu Z. The propagation of lamb waves in a plate bordered with layers of a liquid. J Acoust Soc Am 1992;91:861–7.
[19] Nayfeh AH. Wave propagation in layered anisotropic media. Amsterdam, The Netherlands: Elsevier; 1995.
[20] Shuvalov AL, Poncelet O, Deschamps M. Analysis of the dispersion spectrum of fluid-loaded anisotropic plates: leaky-wave branches. J Sound Vib 2006;296:494–517.
[21] Cegla FB, Cawley P, Lowe MJS. Material property measurement using the quasi-Scholte mode — a waveguide sensor. J Acoust Soc Am Mar. 2005;117:1098–107.
[22] Cegla FB, Cawley P, Lowe MJS. Fluid bulk velocity and attenuation measurements in non-Newtonian liquids using a dipstick sensor. Meas Sci Technol Feb. 2006;17:264–74.
[23] Banerjee S, Kundu T. Ultrasonic field modeling in plates immersed in fluid. Int J Solids Struct Sep. 2007;44:6013–29.
[24] Lamb H. On waves in an elastic plate. Proc R Soc A, Math Phys Eng Sci 1917;93:114–28.
[25] Lowe MJS. Matrix techniques for modeling ultrasonic waves in multilayered media. IEEE Trans Ultrason Ferroelectr Freq Control 1995;42:525–42.

[26] Yu L, Tian Z. Lamb wave structural health monitoring using a hybrid PZT-laser vibrometer approach. Struct Health Monit 2013;12:469–83.
[27] Ruzzene M. Frequency–wavenumber domain filtering for improved damage visualization. Smart Mater Struct 2007;16:2116–29.
[28] Michaels TE, Michaels JE, Ruzzene M. Frequency–wavenumber domain analysis of guided wavefields. Ultrasonics 2011;51:452–66.
[29] Alleyne DN, Cawley P. A two dimensional Fourier transform method for the measurement of propagating multimode signals. J Acoust Soc Am 1991;89:1159–68.
[30] Tian Z, Yu L. Lamb wave frequency–wavenumber analysis and decomposition. J Intell Mater Syst Struct 2014;25:1107–23.
[31] Johnson DH, Dudgeon DE. Array signal processing: concepts and techniques. Upper Saddle River. NJ, USA: Prentice-Hall Inc.; 1993.
[32] Managing gas accumulation in emergency core cooling, decay heat removal, and containment spray systems. NRC Generic Letter 2008-01, January 2008.
[33] Yu L, Shin YJ, Wang J. An ultrasonic guided wave sensor for gas accumulation detection in nuclear emergency core cooling systems. In: 8th international workshop on structural health monitoring. September 10, 2011.